batteries

MDPI

Review

Strategies to Suppress Polysulfide Dissolution and Its Effects on Lithium–Sulfur Batteries

Grace Cheung [1] and Chun Huang [1,2,3,*]

[1] Department of Materials, Imperial College London, London SW7 2AZ, UK
[2] The Faraday Institution, Didcot OX11 0RA, UK
[3] Research Complex at Harwell, Appleton Laboratory, Didcot OX11 0FA, UK
* Correspondence: a.huang@imperial.ac.uk

Abstract: Lithium–sulfur batteries (LSBs), with a high energy density (2600 W h kg^{-1}) and theoretical specific capacity (1672 mA h g^{-1}), are considered the most promising next-generation rechargeable energy storage devices. However, polysulfide dissolution and the shuttle effect cause severe capacity fading and the rapid loss of the active material; hence, these must be addressed first. This review provides an overview of various strategies employed to immobilise polysulfides via polysulfide trapping and physical and chemical adsorption using porous cathode designs, heterostructures, functionalised separators, and polymer binders. The working mechanism of each strategy is reviewed and discussed, highlighting their advantages and disadvantages, and they are analysed through comparisons of the battery performance and limitations in terms of practical applications. Finally, the future prospects for the design and synthesis of LSBs to limit polysulfide dissolution are discussed.

Keywords: lithium–sulfur battery; polysulfide dissolution; shuttle effect

Academic Editor: Shaozhuan Huang

Received: 21 February 2025
Revised: 28 March 2025
Accepted: 31 March 2025
Published: 3 April 2025

Citation: Cheung, G.; Huang, C. Strategies to Suppress Polysulfide Dissolution and Its Effects on Lithium–Sulfur Batteries. *Batteries* **2025**, *11*, 139. https://doi.org/10.3390/batteries11040139

1. Introduction

The significance of sustainable energy systems has increased with the depletion of natural resources like fossil fuels. The growing awareness of the detrimental environmental effects of such fuels, such as CO_2 emissions, has redirected society towards clean and renewable but less reliable alternatives [1,2]. Lithium-ion batteries (LIBs), first commercialised by Sony in 1991, have been highly successful due to their high energy density, long cycle life, and compact size compared to lead–acid batteries [3,4]. However, their high production cost due to cobalt has shifted the demand towards more cost-effective alternatives. Other types of batteries, such as zinc metal batteries [5], sodium ion batteries [6,7], and potassium ion batteries [8,9], as well as potassium dual-ion capacitors [10], have also attracted attention.

Lithium–sulfur batteries (LSBs) have emerged as a promising candidate for rechargeable energy storage due to their high theoretical specific capacity (1672 mA h g^{-1}) and at least three times greater energy density (2600 W h kg^{-1}), provided by their sulfur cathodes [11,12]. These cathodes also offer the additional benefits of being low-cost, naturally abundant, and environmentally friendly [13,14]. However, LSBs still face challenges, including (1) volume changes during lithiation/delithiation [15]. The battery can expand by approximately 80% during lithiation, which can cause contact losses and cracks. (2) The formation of lithium dendrite nucleation sites over time poses safety concerns like internal short circuits, especially with flammable electrolytes [16–19]. (3) The poor intrinsic electronic conductivity of sulfur leads to low active material utilisation [20]. Hence, sulfur is

commonly used alongside conductive hosts like carbon matrices, but lower sulfur content leads to a significant reduction in energy density [21]. (4) Polysulfide intermediates' dissolution results in capacity fading and poor cycle stability, limiting the overall efficiency and longevity of batteries [22]. This review focuses on understanding the fundamental mechanisms of polysulfide dissolution and the strategies used to suppress polysulfide dissolution and shuttle effects, with the goal of achieving the high cyclability and efficiency of LSBs. This review begins by exploring the fundamental working principles of LSBs and the challenges caused by polysulfide dissolution, followed by a detailed examination of recent advancements to suppress polysulfide dissolution and their effects. The advancements are categorised as physical and chemical approaches. The review also considers specific polymer-based binders for the cathodes of LSBs.

2. Overview and Reaction Mechanism of Polysulfide Dissolution and the Problems Associated

Current LSBs suffer from major drawbacks, including the dissolution of intermediate products. During discharge, Li^+ and electrons are released from the Li anode and flow towards the S cathode. Li^+ reduces the cathode to lithium sulfide (Li_2S), following the electrochemical reaction below:

$$S_8 + 16Li + 16e^- \longleftrightarrow 8Li_2S$$

In reality, the sulfur transformation is slower and involves multiple complex steps from longer-chain polysulfides to shorter-chain polysulfides. This behaviour is displayed as two discharge plateaus in a typical profile located approximately at 2.3 V and 2.1 V (Figure 1a). The first plateau corresponds to the reduction of S_8 to Li_2S_4, contributing 25% of the total theoretical capacity. The second plateau, which accounts for the remaining 75%, involves the sluggish stepwise conversion of Li_2S_4 to Li_2S_2 and further to Li_2S [23].

During lithiation, longer-chain polysulfides (Li_2S_n, $4 \leq n \leq 8$) initially form at the cathode. Li_2S_6 and Li_2S_8 are highly soluble in commonly used electrolytes like ether-based electrolytes [24]; other polysulfide species such as Li_2S_4 are also soluble. These polysulfides dissolve in the electrolyte and diffuse to the Li anode, where they are further reduced into insoluble shorter-chain polysulfides. Subsequently, the shorter-chain polysulfides migrate back to the cathode to form longer-chain polysulfides again (Figure 1b) [25]. However, this is not always the case, because shorter-chain polysulfides can be directly reduced or follow a stepwise reduction on the Li anode surface to solid Li_2S or Li_2S_2, forming an insoluble layer. The dissolution of polysulfides results in the irreversible loss of active sulfur material caused by adverse reactions during the continuous cycling of sulfur species between the electrodes. This effect, known as the "shuttle effect", is largely responsible for the degradation of LSBs by causing the continuous loss of sulfur, anode corrosion, low Coulombic efficiency, and poor cycle stability. Self-discharge occurs due to internal chemical reactions; the effective capacity and energy density of the battery are reduced over time after charging, even when the battery is not being used [26]. Adverse reactions at the anode surface lead to the formation of an insoluble layer of lithium sulfide, hindering redox kinetics and affecting the cycling life [27]. Furthermore, utilising high sulfur loading to achieve a high energy density increases the concentration of dissolved intermediates and the electrolyte viscosity, resulting in slower kinetics and a shorter cycle life. Addressing these challenges is crucial in achieving high-energy-density and high-reversibility LSBs.

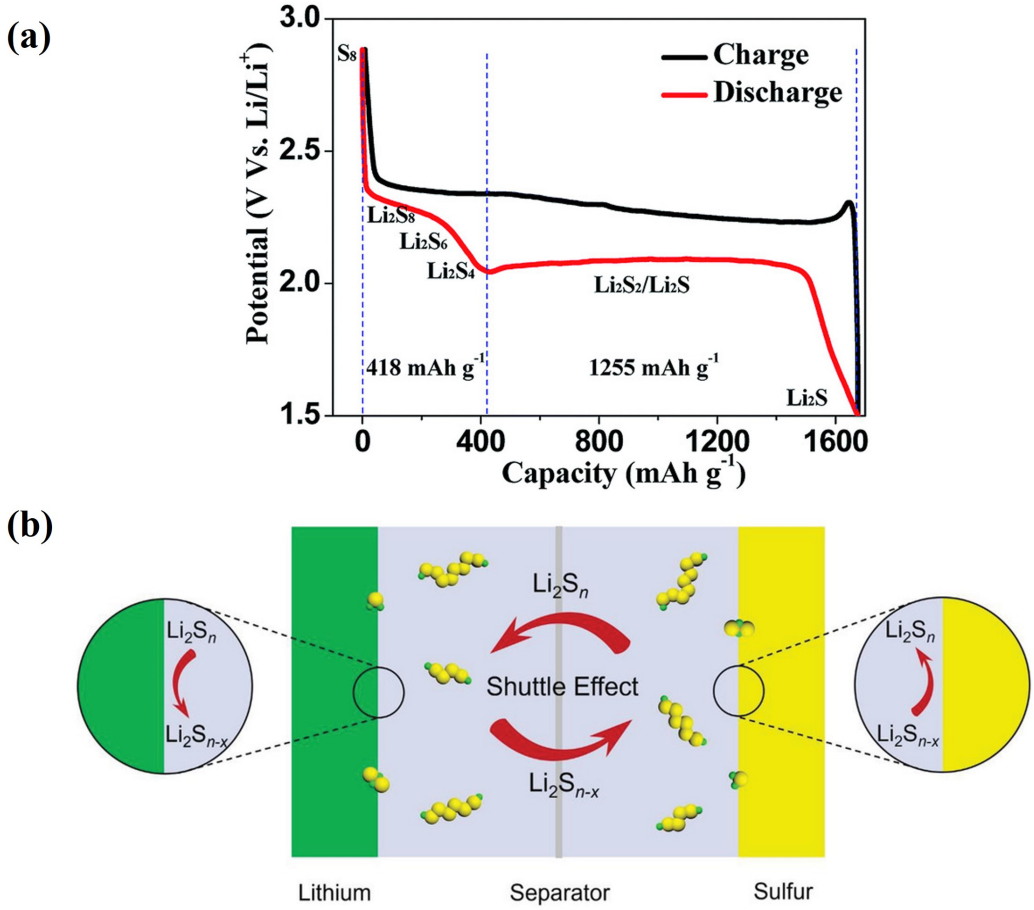

Figure 1. (**a**) Typical charge–discharge profile of a Li-S battery. Reproduced with permission [28]. Copyright 2019, The Royal Society of Chemistry. (**b**) Schematic showing the polysulfide shuttle effect. Reproduced with permission [29]. Copyright 2022, The Authors.

3. Strategies for Polysulfide Trapping and Polysulfide Shuttle Suppression

3.1. Physical Approaches

Physical approaches involve utilising electrolytes to electrostatically repel polysulfides or fabricating cathodes to avoid step-by-step sulfur reduction completely [22,30]. However, in conventional ether-based electrolytes, dissolved polysulfides are essential in delivering Li^+ between electrodes [24]. Another approach explores the structure and sizes to physically confine dissolved polysulfides, thus inhibiting their transfer between electrodes. While this method does not completely prevent the dissolution, it remains applicable in ether-based electrolytes. This section will focus on exploiting the structure and morphology, such as the porosity and shape, to physically encapsulate intermediates.

To tackle these challenges, studies have involved modifying sulfur-carbon cathodes by incorporating porosity into the carbon network [31] and developing carbon composite materials [32]. A suitable level of porosity improves the battery's reversibility by accommodating volume changes during cycling. Additionally, encapsulating polysulfides becomes feasible, thus suppressing migration, while improving the electrical energy provided by the carbon [33].

Polysulfides' encapsulating and electrochemical properties are highly dependent on the pore sizes and structures. For instance, micropores (ranging from 0.7 nm to 1.5 nm) effectively utilise their small geometries to capture polysulfides and sulfur, preventing dissolution in electrolytes [34]. Rao et al. reported a simple entrapment strategy utilising a porous carbon–sulfur composite design prepared using heat treatment with a polyacryloni-

trile (PAN) + polymethyl methacrylate (PMMA) mixture, followed by a chemical deposition method [35]. The pore size achieved was approximately 2 nm (Figure 2a), and electrochemical measurements indicated a stable discharge capacity of over 740 mA h g^{-1} (based on sulfur in the electrode) after 100 cycles at a 0.05 C-rate. However, the sulfur loading was limited to 53.7 wt% due to small pore sizes. Similarly, a sulfur–microporous activated carbon (AC) composite cathode with a smaller pore size of 1.0 nm was reported to successfully capture sulfur within the pores [36]. X-ray diffraction (XRD) and X-ray photoelectron spectroscopy (XPS) results revealed that strong sulfur–carbon interaction was not required to embed nano-sized sulfur within micropores. Furthermore, it displayed stable cycling by retaining a discharge capacity of 1000 mA h g^{-1} after 100 cycles at a 0.1 C-rate. However, limited micropore sizes could only host smaller sulfur molecules, thus again constraining sulfur loading to 29 wt%.

Following this, a different approach to producing a cathode with a high micropore density and large pore volume was investigated [37]. A study on microporous AC derived from azulmic acid precursors, activated at 900 °C, revealed a cathode with smaller pores (Figure 2b), a specific surface area of 2633 m^2 g^{-1}, and a pore volume of 1.286 cm^3 g^{-1}, enabling very high sulfur loading of up to 70 wt% [38]. A large specific surface enhances the efficiency of electrochemical reactions and ion exchange between the electrolyte and electrode. Initially low percentages of lithium-ion utilisation (PLIU) were observed for activation at 800 °C and 900 °C at 65 % and 49 %, respectively (Figure 2c). On average, the cathode with higher sulfur loading (AZC-AZC-K_2CO_3-900-S) exhibited lower PLIU than a cathode with lower loading (AZC-KOH-800-S). This low PLIU is due to the irreversible formation of SEI, which arises from parasitic reactions at the anode surface caused by the increased shuttling effect of polysulfide species at higher sulfur loading [39]. Increasing the porosity, while maintaining small pore sizes (~1 nm), facilitates high sulfur loading and sulfur species confinement within the electrode. Although micropores are highly effective in capturing polysulfides, their complete retention remains challenging at elevated sulfur loadings, as the dissolution into the electrolyte is exacerbated.

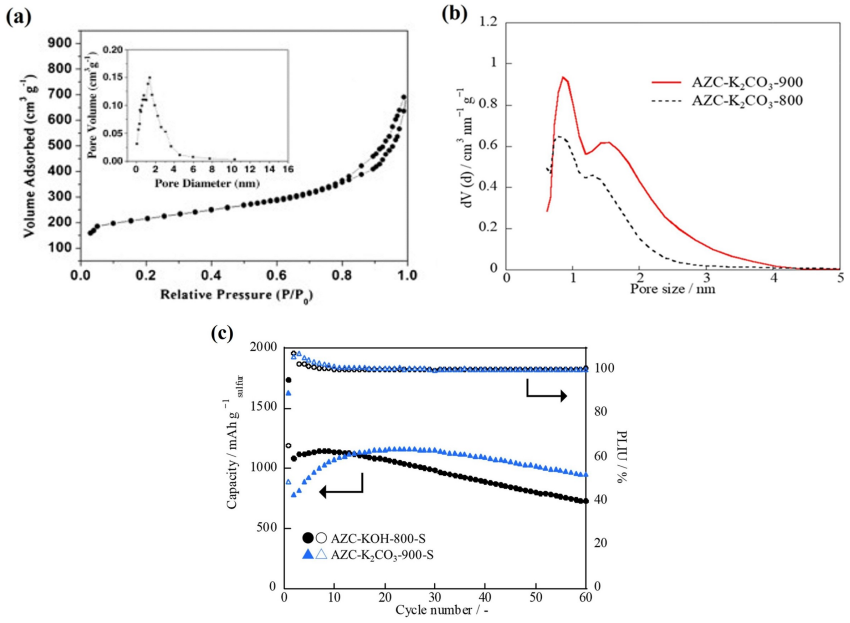

Figure 2. (**a**) Pore size distribution of porous sulfur–carbon composites. Reproduced with permission [35]. Copyright 2012, Elsevier B.V. (**b**) Pore size distribution for AZC-K2CO3-800 and AZC-K2CO3-900 and (**c**) discharge capacity and PLIU % vs. cycle number for AZC-KOH-800-S and AZC-K2CO3-900-S. Reproduced with permission [38]. Copyright 2022, The Authors.

An alternative approach to preventing these issues involves utilising a cathode featuring mesoporosity or macroporosity. The porosity in both cases facilitates the rapid encapsulation of polysulfides and improves ion transport, while accommodating more sulfur [34]. These concepts are commonly used in hierarchical porous carbon hosts to provide a physical barrier to prevent polysulfide dissolution and shuttle effects, while maximising the sulfur content. Exploring this concept, mesoporous silica with various shapes (spherical, rod-like, quasi-hexagon, stripe-like), encapsulated within a reduced graphene oxide shell (RGO-S/SiO_2), was investigated with a polyvinylidene fluoride (PVDF) binder and conventional electrolyte (1M LiTFSI in dimethyl ether (DME)/dioxolane (DOL) at 1:1 ratio) [40]. Reduced graphene oxide (RGO) offers a large specific surface area to facilitate electrochemical reactions, and its layered structure aids in ion transport [41]. In addition, the confined geometry of mesoporous silica enhanced the capillary force, resulting in the better adsorption of polysulfides, as well as aiding the formation of Si-S bonds [42]. TEM showed spherical SiO_2 particles that had disordered pore arrangements and small pore sizes (2.3 nm), while the quasi-hexagonal morphology displayed a more ordered pore arrangement and the largest pore sizes (6.5 nm).

Porous SiO_2 sulfur host cathodes with an RGO outer shell exhibited excellent performance in restricting polysulfides within the pores of SiO_2, using capillary forces to inhibit polysulfide dissolution. RGO provided an extra barrier for escaped polysulfides and helped to suppress polysulfide dissolution by providing additional physical confinement for "leaky" polysulfides. The main physical strategy of optimising the pore size and structure to confine polysulfide dissolution is accompanied by the chemical strategy of the formation of Si-S bonds between Li_2S_4 and SiO_2 and interactions between S- and O-containing functional groups, which improved the chemical adsorption of polysulfide species and further suppressed polysulfide dissolution [42]. Thermogravimetric analysis (TGA) revealed that spherical-shaped S/SiO_2 particles had the lowest sulfur content of 21 wt% after sulfur impregnation. In comparison, quasi-hexagon had the highest of 76 wt% due to limitations in sulfur crystallisation. The synergistic effects of the multiple strategies resulted in the spherical SiO_2 displaying the best cell performance, with an initial capacity of 1484 mA h g^{-1} and a final capacity of 1122 mA h g^{-1} after 200 cycles at a 0.1 C-rate. Very stable long-term cycling performance was also achieved over 500 cycles, making it very suitable for practical applications. On the other hand, the quasi-hexagon with the highest sulfur loading achieved a capacity of 603 mA h g^{-1} after 200 cycles at a 0.1 C-rate, with an initial capacity of 1041 mA h g^{-1}. The differences in performance may be attributed to the higher disorder in spherical particles, which enhanced the chemical adsorption and trapping of polysulfides with the main physical confinement. To summarise, the RGO-encapsulated mesoporous silica architecture was able to adsorb polysulfides and achieved a high initial discharge capacity approaching its theoretical capacity (1567 mA h g^{-1} at 0.1 C) and stable cycle performance, with a capacity loss of only approximately 0.05% per cycle, demonstrating the advantages of the physical approach [40]. However, the porous SiO_2 particles with RGO capsulation exhibited a relatively low density due to the pores inside the particles, which may reduce the volumetric energy densities. Furthermore, although spherical particles displayed the best stability and long-term performance, the sulfur loading content was limited to only 21 wt% (compared with 76 wt% for quasi-hexagon particles), which may lead to lower energy densities at the battery cell level.

3.2. Chemical Approaches

Chemical approaches aim to immobilise intermediates through chemical interactions by utilising the chemical bonding and chemical affinity of functional groups. These approaches offer alternative strategies to physically confine polysulfides by trapping them

via chemical adsorption. In addition to the functional materials, electrocatalysts play a significant role by aiding the conversion of lithium polysulfides and lowering the activation energy required for these processes. By integrating chemical adsorption mechanisms with catalytic activity, these strategies enhance the electrochemical performance and overall stability of LSBs.

3.2.1. Catalytic Material for Polysulfide Conversion

Dissolved lithium polysulfides are the primary reason for sluggish reaction kinetics in LSBs. As previously noted, the process of sulfur transformation involves complex steps and becomes increasingly difficult due to the high activation energy required. To tackle this issue, electrocatalysts have been employed to lower the energy barriers and speed up the conversion of Li_2S [43,44]. Heterostructure designs enables electronic tuning and the optimisation of coordination environments, thereby improving the electrochemical performance of LSBs via the "adsorption–catalysis" synergistic effect, which the traditional homogeneous interfaces cannot achieve [45]. By increasing the conversion rate of soluble polysulfides, the accumulation of long-chain polysulfides and the irreversible loss of active sulfur can be minimised. Recently, an interesting study by Azam et al. reported an environmentally friendly interlayer produced from cellulose-derived carbon cloth, combined with CeO_2 nanorods, which demonstrated enhanced catalytic conversion properties for lithium polysulfides and high capacity retention [46]. The incorporation of cellulose, a material that is both abundant and cost-effective, provides a significant advantage to this approach. Polar materials such as metal carbides, metal oxides, metal sulfides, and metal nitrides [47–51], and composite materials such as $MoTe_2$@graphene [51], can exhibit strong interactions with polysulfides, effectively suppressing the shuttle effect without requiring additional modifications. For example, recent studies have involved the use of NiS_2-$NiSe_2$, FeS_2-MnS, Sc_2CO-MXene/*h*-BN, NiS_2-WS_2 heterostructures to enhance the adsorption capacity and anchoring ability of polysulfides [52–55]. These heterostructures can effectively inhibit the shuttle effect caused by polysulfide dissolution while facilitating high sulfur loading.

Amongst these options, cobalt-based materials have demonstrated outstanding catalytic conversion abilities and strong adsorption properties towards polysulfides, thereby significantly improving the reversibility of LSBs. Furthermore, cobalt sulfides have higher electrical conductivity compared to cobalt oxides, thus allowing easier charge transfer during lithiation/delithiation processes [56]. For instance, Zhang et al. prepared CoS_2 nanoribbons via a solvothermal method, followed by in situ sulfurisation to create a CoS_2-$CoSe_2$ heterostructure catalyst design [57]. A change in the coordination environment of Co sites was observed owing to phase transition into a metastable orthorhombic phase upon sulfurisation. Improved catalytic conversion and increased adsorption sites from this phase transition were evidenced by UV–vis and visual adsorption tests (Figure 3a,b). The battery employing the CoS_2-$CoSe_2$ separator demonstrated a higher capacity of 612 mA h g^{-1} after 400 cycles at a 1 C-rate compared to an individual $CoSe_2$ battery (353 mA h g^{-1}). Furthermore, cyclic voltammetry revealed a higher current density in CoS_2-$CoSe_2$, indicating the successful acceleration of polysulfide conversion. Similarly, a functionalised separator of Co/MXene-derived TiO_2 (Co@M-TiO_2/C) was developed by Chang et al. [58] via a facile hydrothermal method and calcination, incorporating both a porous structure and heterostructure. This provided a large contact area for active sites, exhibited good electrical conductivity, and demonstrated catalytic effects on polysulfides. The Co@M-TiO_2/C separator possessed excellent cycle stability even at high sulfur loading of 4.4 mg cm^{-2} and a discharge rate of 2 C after 300 cycles with an initial capacity of 1481.71 mA h g^{-1} (Figure 3d). Furthermore, cyclic voltammetry curves revealed lower polarisation in Co@M-TiO_2/C and larger redox peaks, indicating the rapid diffusion of ions (Figure 3c).

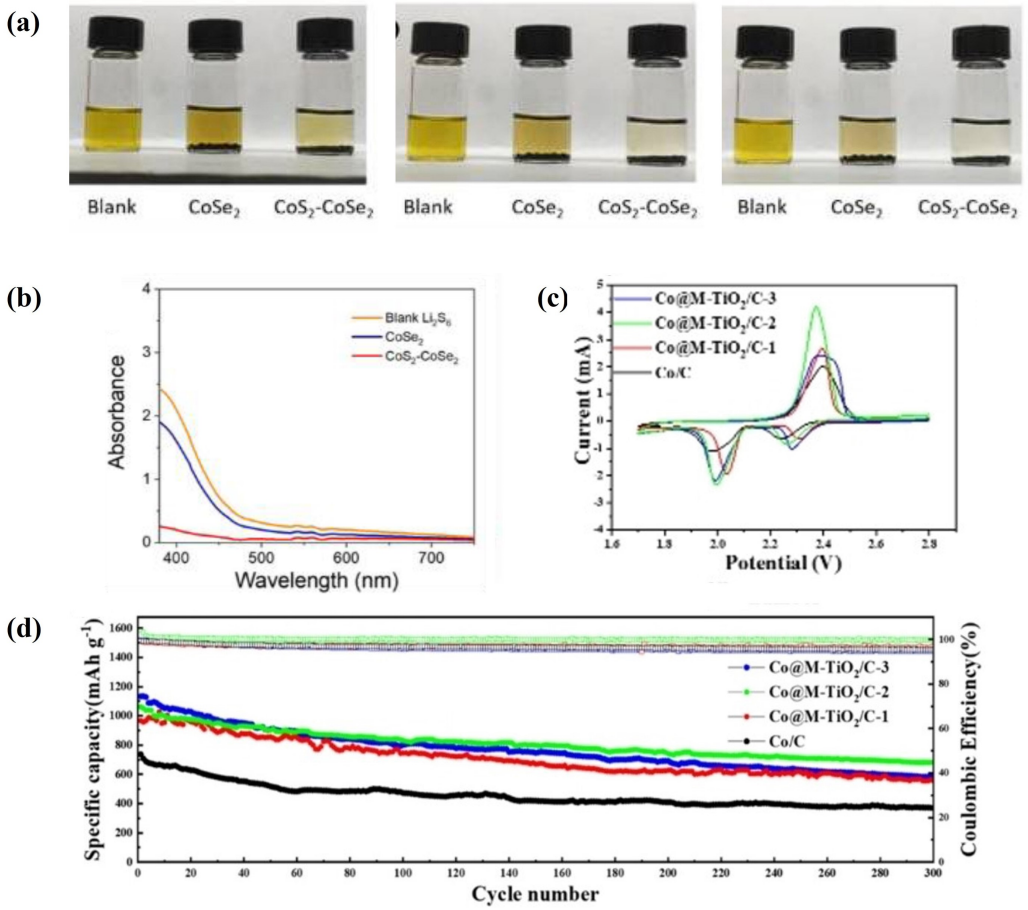

Figure 3. (**a**) Li_2S_6 adsorption test photographs for 0.5 h, 3 h, 5 h (starting from the left) and (**b**) UV–vis spectra of Li_2S_6 solution after 5 h of adsorption with $CoSe_2$ and CoS_2-$CoSe_2$. Reproduced with permission [57]. Copyright 2023, The Authors. (**c**) Cycle performance at 1 C-rate and (**d**) CV curves for different Co@M-TiO_2/C samples and Co/C. Reproduced with permission [58]. Copyright 2023, The Authors.

Following this, the introduction of a built-in electric field can accelerate electron transfer and the redistribution of charge, promoting polysulfide conversion and adsorptivity [59]. This method mitigates sluggish reaction kinetics while impeding the shuttle effect. The presence of Co–metal electron donors can induce negative charges on the adjacent material, enhancing its ability to adsorb positive polysulfides. At thermodynamic equilibrium, Mott–Schottky heterojunctions induce a built-in electric field due to differences in energy levels and electron affinities (Figure 4). Recently, Zheng et al. predicted, using density functional theory (DFT) calculations, strong binding energy and adsorption abilities for polysulfides, accompanied by fast electron transfer for polysulfide conversion facilitated by the metallic behaviour exhibited at the Co/CoS_2 MS heterostructure [60]. A N, S-co-doped carbon nanocage implanted with Co/CoS_2 (Co/CoS_2@NC) was synthesised to enhance conversion and immobilisation by encapsulating CoZn-ZIF in a polydopamine (PDA) layer to allow self-dissolution, followed by carbonisation and sulfurisation (Figure 5a). The resulting N, S-co-doped carbon exhibited strong chemical anchoring to polysulfides, thus delivering a stable capacity of 675 mA h g^{-1} after 500 cycles at a 1 C-rate (Figure 5c). Similarly, Zhu et al. reported a catalyst comprising N-doped carbon with a Co/W_3N_4 heterojunction (Co/W_3N_4@NC) featuring a strong built-in electric field (Figure 5b) [61]. UV–vis spectra revealed a strong Li_2S_6 adsorption capacity in the Co/W_3N_4 heterojunction compared to the Co/$W_{4.6}N_4$ heterojunction, which exhibited weaker built-in electric field strength. The reported Co/W_3N_4@NC cathode displayed excellent reversibility (791.5 mA h g^{-1}

after 500 cycles at 1 C-rate), cycle stability at high sulfur loading of 5.5 mg cm^{-2}, and a high initial specific capacity of 1313.6 mA h g^{-1}, with 97.4 % capacity retention (Figure 5d). Mott–Schottky heterostructures effectively suppress the effects of polysulfide dissolution by promoting the redistribution of charge via built-in electric fields, thereby facilitating chemical adsorption and enhancing the electric conductivity for polysulfide conversion.

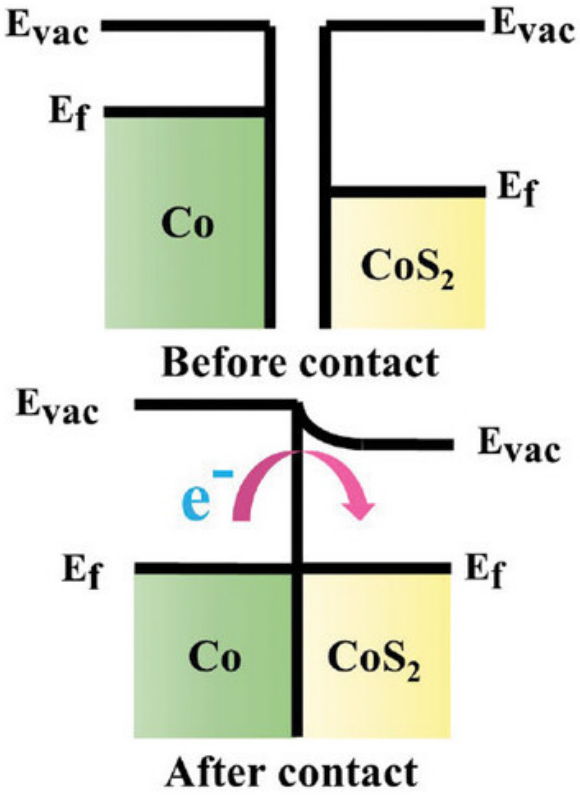

Figure 4. Schematic illustration of Co and CoS_2 before and after contact, showing the flow of electrons. Reproduced with permission [60]. Copyright 2023, Wiley.

The sulfur reduction reaction (SRR) facilitates up to 16 electrons; however, its sluggish reaction kinetics restrict LSBs' capacities and cycling life. In particular, the conversion of polysulfides into insoluble Li_2S_2/Li_2S requires much higher activation energy than the conversion of sulfur to soluble polysulfides [62]. Hence, the SRR requires efficient electrocatalysts. As an SRR catalyst, heteroatom-doped graphene has been explored, where the experimental results showed that nitrogen and sulfur dual-doped graphene considerably reduced the activation energy and improved the SRR kinetics, corroborating DFT simulation results that showed that the doping tuned the *p*-band centre of the active carbons for the optimal adsorption strength regarding intermediates and electroactivity [62,63]. The pivotal role of radicals was comprehensively explored using ultrathin nitrogen–oxygen co-doped carbon nanosheets, where the abundant N-O active sites synergistically anchored LiS_3* radicals, facilitating efficient multi-pathway sulfur conversion [64]. Metal–nitrogen-doped carbon SRR catalysts were investigated, and anchoring FeNCs onto carbon filters for the sulfur cathode resulted in an enhanced cycle life of over 10,000 h for LSBs [65]. Specifically, polysulfide adsorption–desorption and the electrochemical conversion kinetics varied with the incremental addition of even a single Fe atom to the catalyst metal centre [66]. The metal centre with exactly two Fe atoms represents the optimal configuration, maximising the atom utility and adeptly handling the conversion of varied intermediate sulfur species [66]. Finally, an effective and simple screening descriptor for high-throughput material screening, i.e., the one-dimensional density of states (1D-DOS)

fingerprint similarity, was developed to identify potential SRR catalysts. This method effectively distinguished and identified 30 potential candidates for the SRR from 420 types of MXene [67].

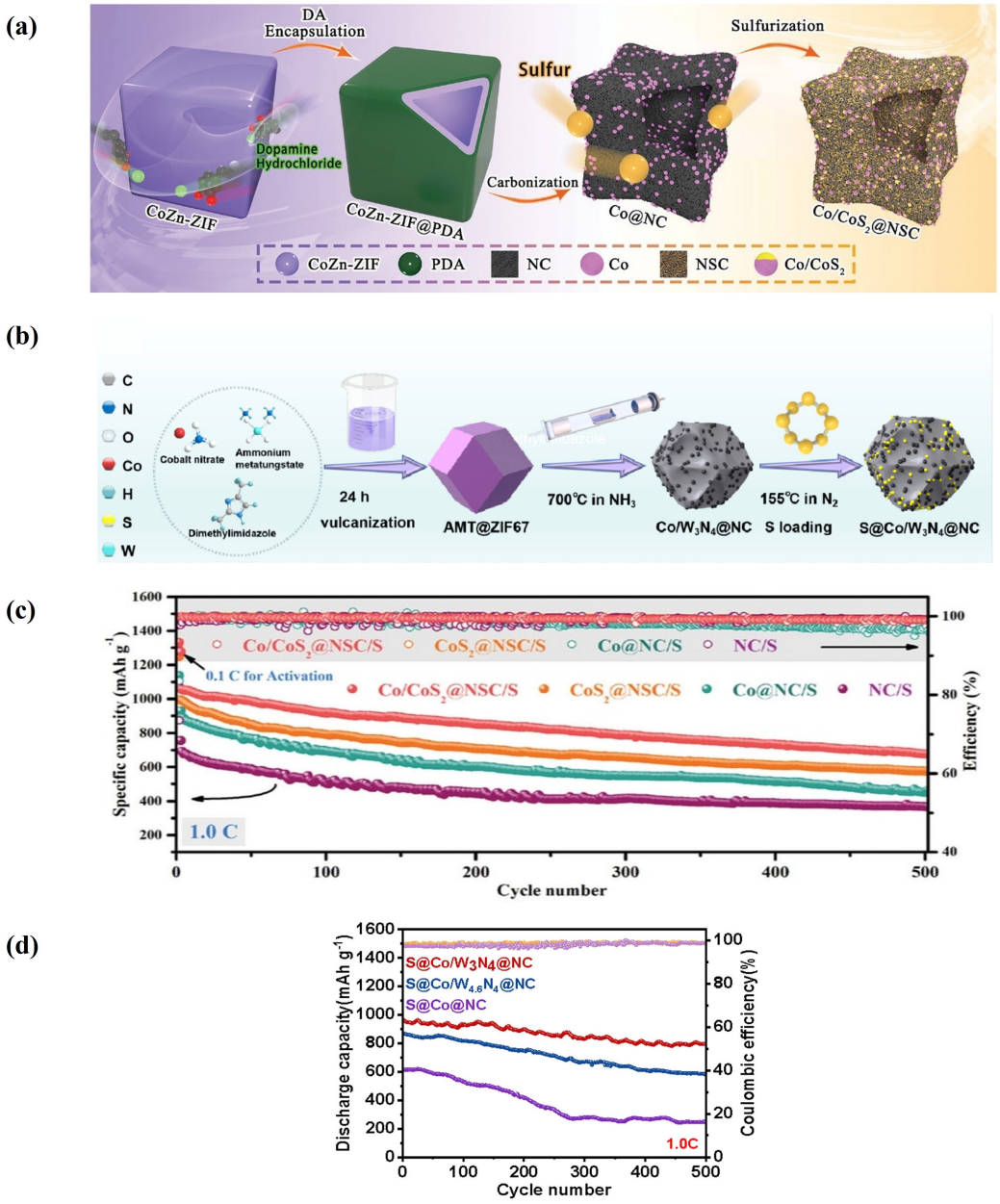

Figure 5. Schematic diagram of the synthesis of (**a**) Co/CoS_2@NC and (**b**) Co/W_3N_4@NC. Cycle performance over 500 cycles at 1 C-rate for (**c**) Co/CoS_2@NC and (**d**) Co/W_3N_4@N. (**a**,**c**) Reproduced with permission [60]. Copyright 2023, Wiley. (**b**,**d**) Reproduced with permission [61]. Copyright 2024, Elsevier Ltd.

3.2.2. Separators

Typically, high-energy-density LSBs are achieved by maximising the sulfur loading and utilisation. However, the shuttle effect is significantly exacerbated by this, and separators play a crucial role in minimising this effect. Separators are also essential to avoid short circuits by providing a physical and electronically insulating layer of barrier between the anode and cathode. Conventional separators used in LSBs are typically derived from polymeric materials such as polyethylene (PE) and polypropylene (PP) [68]. However, these are ineffective in anchoring soluble polysulfides owing to the non-polarity of the materials [69]. To overcome this problem, studies have involved functionalising separators

with polar materials. Lin et al. reported a PP-modified separator design, consisting of porous CoP/C nanocubes that had a strong chemical affinity with lithium polysulfide [70]. Large active surfaces were provided by the porous structure (Figure 6a), thus facilitating fast lithium-ion diffusion and effective polysulfide anchoring by the formation of Co-S bonds. In addition, cyclic voltammetry at different scanning rates demonstrated rapid liquid-phase polysulfide conversion at the interface via improved redox kinetics owing to the lower resistance of CoP/C. The shortened lifespans of longer-chain polysulfides mitigated the shuttle effect, improved the battery performance, and reduced capacity loss [71]. Stable cycling performance was achieved at higher sulfur loadings (3.2 mg cm^{-2}), retaining 601.3 mA h g^{-1} after 100 cycles at a 0.5 C-rate (Figure 6b).

Another study employing a TiN synergetic hierarchical 3D micro-/mesoporous carbon separator (MMC-TiN) by Tang et al. enabled high physical adsorption and high lithium ion diffusion through a mixture of pore sizes, i.e., 1.27 nm and 5.30 nm [72]. The large specific surface area of 1571 m^2 g^{-1} further suppressed polysulfide dissolution by chemically immobilising the longer-chain polysulfides through polarity. The chemical adsorption of polysulfides prevents the deposition of insoluble sulfur species on the anode, avoids an increase in electrolyte viscosity, and impedes the shuttle effect, enabling high sulfur loading. However, evaluations of the practical viability over 400 cycles revealed a significant limitation caused by crack formation during cycling. The coating degradation reduced the battery capacity to just 500 mA h g^{-1} after 400 cycles at a 1 C-rate.

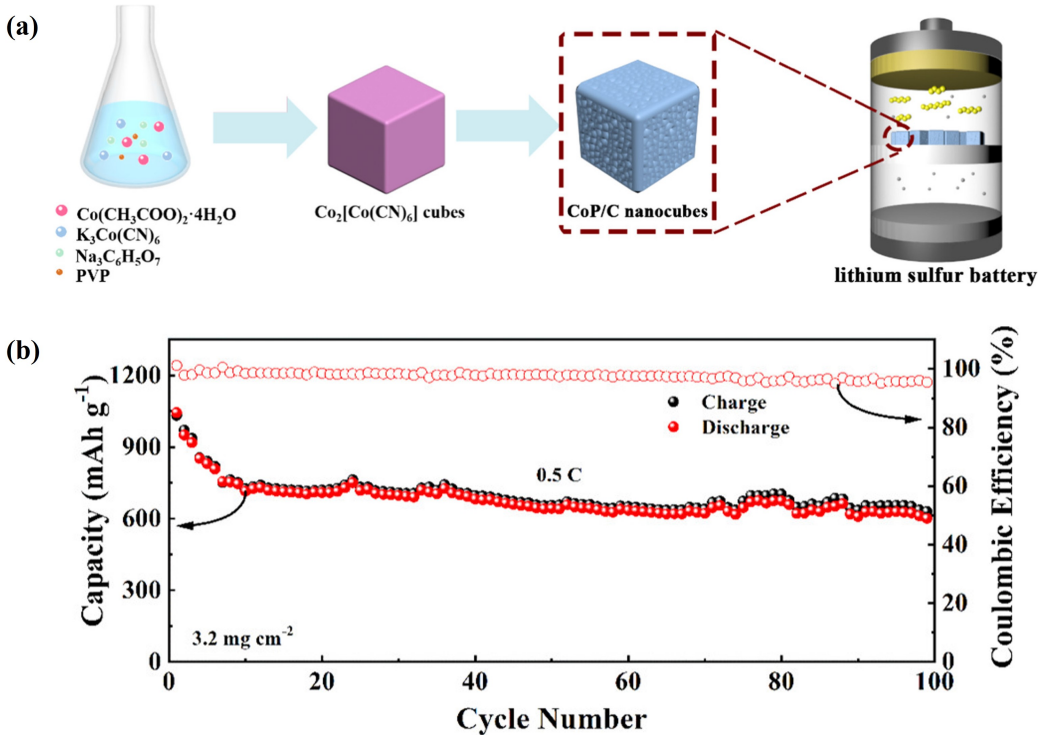

Figure 6. (**a**) Schematic showing a CoP/C nanocube PP-modified separator and (**b**) the cycle performance of high-sulfur-loading CoP/C nanocubes. Reproduced with permission [70]. Copyright 2019, American Chemical Society.

3.2.3. Polymer-Based Binders

PVDF is the most commonly used binder in LSBs owing to its good electrochemical stability [73]. However, PVDF binders are not suitable for use in high-sulfur-loading environments because they have a weak affinity for lithium polysulfides and relatively low adhesion strength, and they are insulating and cannot promote active sulfur utilisation [74–78].

A study on a bifunctional binder with linear polyethylene glycol (PEG) and nucleophilic maleate-capped ends by Han et al. demonstrated impressive cyclability at ultra-high sulfur content (80 wt%) using a tandem cell configuration (M80S cell) [79]. The maleate ends aided the entrapment of excess polysulfides via C-S interactions. In addition, the linear PEG provided flexibility for high sulfur loading while preventing capacity fading by maintaining electrochemical contact. Cyclic voltammetry revealed excellent battery reversibility as well as good reaction kinetics and sulfur utilisation, suggesting highly effective polysulfide immobilisation (Figure 7a). At 80 wt% sulfur, the battery retained 522 mA h g^{-1} after 200 cycles at a 0.2 C-rate, with an initial capacity of 1102 mAh g^{-1}. However, the capacitor loss became increasingly large after 100 cycles, and the capacitor retention decreased from 82% to 58% in only 50 cycles (Figure 7b).

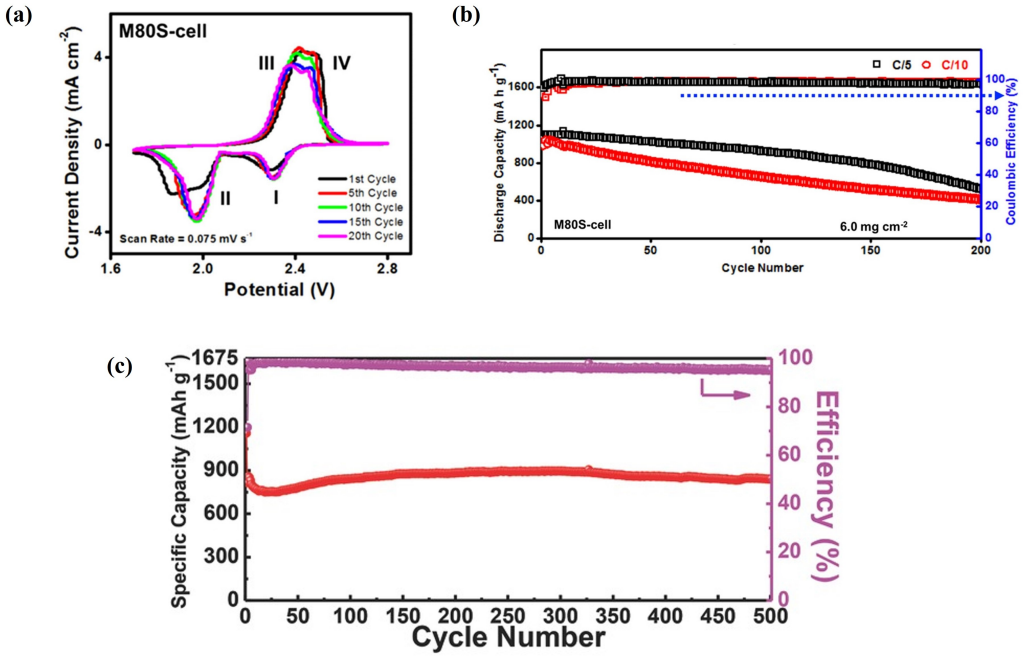

Figure 7. (**a**) CV curves and (**b**) cycle performance at different C-rates of M80S cell. Reproduced with permission [79]. Copyright 2019, American Chemical Society. (**c**) Long-term cycling of S@GA. Reproduced with permission [80]. Copyright 2015, Wiley.

Using a similar mechanism, Li et al. studied bio-derived aqueous polymer binders with rich functional groups (gum arabic, GA) to improve the longevity of LSBs [80]. The S@GA cathode was fabricated using a green aqueous process without the use of toxic organic solvents. GA, rich in polysaccharides and glycoproteins, offers abundant functional groups, including hydroxyls that facilitate bonding. X-ray absorption spectroscopy (XAS) and Fourier transform infrared (FTIR) spectroscopy confirmed the formation of C-S bonds and chemical bonds between these functional groups and S. These chemical reactions aided in trapping polysulfides within the cathode, resulting in low material loss and remarkable long-term cycling. Although the sulfur loading (75 wt%) was lower than in the previous strategy, the GA binder exhibited highly stable cycling performance over 500 cycles, retaining 841 mA h g^{-1} at a 0.2 C-rate (Figure 7c).

3.2.4. Comparison of Different Strategies for Mitigation of Polysulfide Dissolution and Shuttle Effects

The physical approach of optimising the pore structures and sizes is an effective method to confine dissolved polysulfides. Achieving higher sulfur content and mass loading is crucial in surpassing the specific energy densities of LIBs. The sulfur content in the cathode structures fabricated by the physical approaches depends on the impregna-

tion methods employed. The most common approach, melt diffusion, involves melting sulfur and diffusing it through the outer porous shell structure [81,82]. Alternatively, the dissolution–diffusion method dissolves sulfur in a solvent and utilises increased capillary pressure to drive its diffusion. However, both mentioned methods require additional high-temperature treatments to eliminate external sulfur accumulation, further escalating the fabrication costs and complexity [83]. The physical encapsulation techniques discussed in Section 3.1 are often costly and involve complex, multiple-step fabrication processes, particularly when dealing with hierarchical structures, making them challenging to scale up for large-scale production.

The approach of using functionalised materials and heterostructures for chemical adsorption has proven highly effective in impeding shuttle effects via their synergistic adsorption–catalysis effects. Chemical adsorption methods are generally stronger and more effective than physical containment methods due to the formation of chemical bonds. Many of these advancements were initially predicted using DFT calculations and subsequently validated by electrochemical characterisation. However, the precise mechanism behind the fast electron transfer and adsorption abilities of heterostructures is not understood completely. Consequently, it is essential to understand and explore these mechanisms further to achieve the commercialisation of LSBs. Furthermore, the functionalised materials and heterostructure designs exhibit variations in their mechanical properties, thermal properties, and structural stability under operational conditions. Some of the materials may not be compatible, which can result in uneven degradation and varying degradation pathways within a working LSB. Lastly, the usage of expensive and scarce materials such as cobalt also limits their commercial viability.

Functionalised separators offer a promising approach to preventing the dissolution of polysulfides by enhancing the conversion rates while immobilising polysulfides through adsorption on the separator. Although functionalised separators have achieved excellent cycling stability, cobalt is still used in some of the functional materials, contradicting the initial idea of using sulfur, which is cost-effective, non-toxic, and highly abundant. Furthermore, this approach comes with other trade-offs, such as an increased battery weight, potential increases in the internal resistance of the battery, and compatibility issues with other battery components. Finally, functionalised polymer-based binders are also an effective approach to suppressing polysulfide dissolution, providing stable cycling and environmental friendliness. This approach is highly compatible with the existing processing method for the cathodes of LSBs. However, the polymer binders usually reduce the electrical conductivity of the cathodes, hence reducing the sulfur utilisation in the cathode. These disadvantages underscore the need for further research to improve their practicality and feasibility for broader applications.

4. Conclusions and Future Directions

LSBs are a promising candidate for rechargeable energy storage following LIBs. However, they still encounter significant obstacles, preventing the exploitation of their full potential for commercialisation. In this review, the different methods employed to suppress polysulfide dissolution and the shuttle effect were explored black (summarised in Figure 8). Initially, strategies utilising porous structures to encapsulate polysulfides within the cathode were evaluated. The synergistic impact of heterostructures on the shuttle effect was discussed, with a particular focus on cobalt-based materials and their performance with other materials at heterojunctions, analysed through theoretical and experimental methods. Secondly, the role of separators in LSBs and the principle by which functionalised separators alleviate the shuttle effect were outlined. Finally, the advantages of using polymer-based binders and their limitations were discussed.

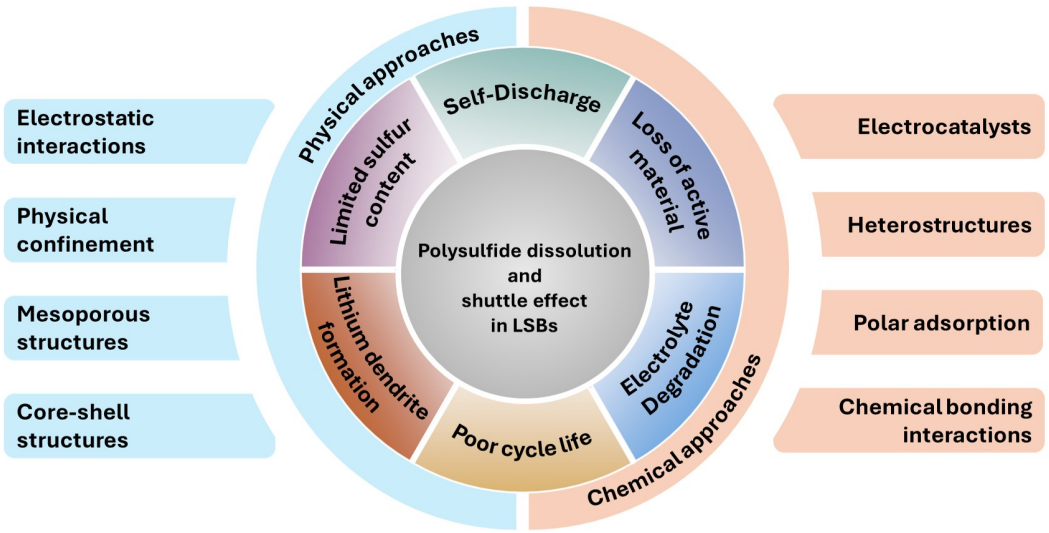

Figure 8. Summary of the approaches employed to suppress polysulfide dissolution and shuttle effects.

Porous cathodes with small pore sizes effectively confine soluble polysulfides compared to large pore sizes. This reduces the migration of polysulfides while enhancing the electrical conductivity of the electrode. However, limitations on high sulfur loading arise when hosting large sulfur molecules in small pores. This challenge can be addressed by employing highly porous materials with large pore volumes encapsulated within an RGO shell. Heterostructures have also attracted attention recently for their strong ability to adsorb polysulfides and catalyse polysulfide conversion, owing to their built-in electric fields and rapid ion diffusion. A stronger built-in electric field can facilitate large polysulfide adsorption. Furthermore, heterostructures and porous structures have demonstrated synergistic effects in achieving excellent LSB properties. Controlling factors such as the electrical conductivity, pore volumes, electronic structures, and size is crucial to suppress polysulfide dissolution and shuttle effects. Chemical approaches utilise specific chemical groups to bind strongly to polysulfides, anchoring them and preventing dissolution. CoP/C separators are superior in impeding the shuttle effect owing to their strong chemical affinity and low resistance, offering stable cycling under high sulfur loading. Polymer-based binders offer potential for high reversibility and efficiency, while maintaining environmental friendliness.

However, the development of LSBs incorporating the above approaches still faces some challenges before commercialisation.

(1) The optimisation and compatibility of materials. The materials must be carefully studied to ensure that their stability and mechanical qualities are sustained during battery operation. The thermal properties, mechanical properties, and structural stability need careful consideration when selecting materials.
(2) Mechanism behind synergistic effects in heterostructures. A deeper understanding of the mechanism underlying the adsorption–catalytic process is crucial in selecting materials with both enhanced catalytic and adsorption activity. This understanding is essential in improving the overall effectiveness of heterostructures in impeding the shuttle effect, as well as the performance of LSBs.
(3) The scalability of synthesis for mass production. While porous structures show promising effects, creating uniform and stable porous structures at nanoscales can be challenging and costly. The complex fabrication processes for heterostructures further add to the costs and complexity, limiting the commercial viability of LSBs. Exploring cost-effective materials and synthesis methods is critical for the commercialisation of LSBs.

(4) Exploring alternatives materials outside of cobalt-based materials. While cobalt-based materials offer high stability and strong adsorption capabilities regarding polysulfides, the usage of cobalt raises concerns associated with environmental impacts, ethical issues, toxicity, and cost-effectiveness, limiting the production of LSBs.

Considering these outlined challenges, some future prospects are summarised here. Porous structures demonstrate effectiveness in physical encapsulation, while heterostructures enable catalysed redox reactions and chemical methods allow strong anchoring via chemical adsorption. Holistic approaches combining both physical and chemical approaches can provide a strategy to suppress polysulfide dissolution and the shuttle effect. The continued exploration of different material systems and the adsorption–catalytic mechanism offers additional perspectives for further improvements. Furthermore, developing less complex, scalable, and streamlined synthesis techniques is vital in achieving commercial feasibility. In summary, porous cathode designs, heterostructures, functionalised separators, and polymer binders significantly suppress polysulfide dissolution and its adverse effects in LSBs, thereby improving their cycle performance, efficiency, and longevity. While significant progress has been made, some areas still require deeper investigation. Specifically, unravelling the mechanism behind the synergistic effects in heterostructures is essential. A closer look at the adsorption–catalytic process can help researchers in identifying materials and structures with superior catalytic and adsorption properties. Such insights will pave the way for designs that minimise the shuttle effect and enhance battery performance, surpassing that of state-of-the-art LIBs. Furthermore, the scalability of synthesis methods for mass production remains a major hurdle. Developing cost-effective and uniform fabrication techniques is essential to transition LSBs from laboratory research to commercial products. Addressing these challenges would mark the first step towards the commercialisation of LSBs.

Author Contributions: Conceptualization, C.H.; software, G.C.; resources, C.H.; writing—original draft preparation, G.C.; writing—review and editing, C.H.; visualization, G.C.; supervision, C.H.; funding acquisition, C.H. All authors have read and agreed to the published version of the manuscript.

Funding: C.H. acknowledges funding from the ERC Starting Grant (converted to UKRI funding EP/Y009908/1), the Faraday Institution research programme grants FIRG060 and FIRG066, the Faraday Institution Industry Fellowship FIIF015, Imperial College London UKRI Impact Acceleration Account EP/X52556X/1, and UKRI EPSRC UKRI Innovation Fellowship EP/S001239/1, EP/S001239/2.

Conflicts of Interest: These authors declare no conflicts of interest.

References

1. Mitali, J.; Dhinakaran, S.; Mohamad, A.A. Energy Storage Systems: A Review. *Energy Storage Sav.* **2022**, *1*, 166–216. [CrossRef]
2. Huang, C.; Wilson, M.D.; Cline, B.; Sivarajah, A.; Stolp, W.; Boone, M.; Connolley, T.; Leung, C.L.A. Li+ concentration and morphological changes at the anode and cathode interphases inside solid-state lithium metal batteries. *J. Phys. Energy* **2025**, *7*, 025009.
3. Blomgren, G.E. The Development and Future of Lithium Ion Batteries. *J. Electrochem. Soc.* **2016**, *164*, A5019–A5025. [CrossRef]
4. Min, G. 11—Power Supply Sources for Smart Textiles. In *Smart Clothes and Wearable Technology*; McCann, J., Bryson, D., Eds.; Woodhead Publishing Series in Textiles; Woodhead Publishing: Sawston, UK, 2009; pp. 214–231. [CrossRef]
5. Gong, Z.; Liu, Z.; Gao, X.W.; Chen, N.; Song, Y.; Wu, X.; Hu, A. Constructing cyclic hydrogen bonding to suppress side reactions and dendrite formation on zinc anodes. *Chem.–Eur. J.* **2024**, *30*, e202402558.
6. Liu, Z.; Song, Y.; Fu, S.; An, P.; Dong, M.; Wang, S.; Lai, Q.; Gao, X.W.; Luo, W.B. Multiphase manganese-based layered oxide for sodium-ion batteries: Structural change and phase transition. *Microstructures* **2024**, *4*, 2024036.
7. Huang, L.; Barker, K.; Liu, X.; Jian, Y.; Skinner, S.J.; Ryan, M.P.; Huang, C. A mixed-anion strategy for constructing rapid ion-conducting Na solid-state electrolyte. *Chem. Inorg. Mater.* **2025**, *6*, 100102.

8. Liu, Z.; Li, S.; Mu, J.; Zhao, L.K.; Gao, X.W.; Gu, Q.; Wang, X.C.; Chen, H.; Luo, W.B. Element-tailored quenching methods: Phase-defective K0. 5Mn1-xCrxO2 cathode materials for potassium ion batteries. *Mater. Today Chem.* **2024**, *40*, 102251.
9. Liu, Z.; Gong, Z.; He, K.; Qiu, P.; Wang, X.C.; Zhao, L.K.; Gu, Q.F.; Gao, X.W.; Luo, W.B. Developments and prospects of carbon anode materials in potassium-ion batteries. *Sci. China Mater.* **2024**, 1–16.
10. Liu, Z.M.; Wang, D.; Li, S.Z.; Lai, Q.S.; Yang, D.R.; Zhao, L.K.; Mu, J.J.; Wang, X.C.; Gao, X.W.; Luo, W.B. An ultrafast rechargeable hybrid potassium dual-ion capacitor based on carbon quantum dot@ ultrathin carbon film cathode. *Rare Met.* **2024**, *43*, 5070–5081.
11. Manthiram, A.; Fu, Y.; Chung, S.H.; Zu, C.; Su, Y.S. Rechargeable Lithium–Sulfur Batteries. *Chem. Rev.* **2014**, *114*, 11751–11787. [CrossRef]
12. Li, M.; Jafta, C.J.; Belharouak, I. 5—Progress of Nanotechnology for Lithium-Sulfur Batteries. In *Frontiers of Nanoscience*; Raccichini, R., Ulissi, U., Eds.; Elsevier: Amsterdam, The Netherlands, 2021; Nanomaterials for Electrochemical Energy Storage; Volume 19, pp. 137–164. [CrossRef]
13. Mori, R. Cathode Materials for Lithium-Sulfur Battery: A Review. *J. Solid State Electrochem.* **2023**, *27*, 813–839. [CrossRef]
14. Haridas, A.K.; Huang, C. Advances and Challenges in Tuning the Reversibility & Cyclability of Room Temperature Sodium–Sulfur and Potassium–Sulfur Batteries with Catalytic Materials. *Mater. Today Energy* **2023**, *32*, 101228. [CrossRef]
15. Shojaei, M.J.; Sivarajah, A.; Safdar, T.; Magdysyuke, O.V.; Leung, C.L.A.; Huang, C. Advanced battery cathode microstructure analysis through operando synchrotron X-ray tomography and super-resolution deep learning. *Solid State Ionics* **2025**, *422*, 116818. [CrossRef]
16. Liu, Y.; Elias, Y.; Meng, J.; Aurbach, D.; Zou, R.; Xia, D.; Pang, Q. Electrolyte Solutions Design for Lithium-Sulfur Batteries. *Joule* **2021**, *5*, 2323–2364. [CrossRef]
17. Huang, C.; Wilson, M.D.; Cline, B.; Sivarajah, A.; Stolp, W.; Boone, M.N.; Connolley, T.; Leung, C.L.A. Correlating Lithium-Ion Transport and Interfacial Lithium Microstructure Evolution in Solid-State Batteries during the First Cycle. *Cell Rep. Phys. Sci.* **2024**, *5*, 101995. [CrossRef]
18. Leung, C.L.A.; Wilson, M.D.; Connolley, T.; Huang, C. Mapping of Lithium Ion Concentrations in 3D Structures through Development of in Situ Correlative Imaging of X-ray Compton Scattering-Computed Tomography. *Synchrotron Radiat.* **2024**, *31*, 888–895. [CrossRef]
19. Huang, C.; Leung, C.L.A.; Leung, P.; Grant, P.S. A Solid-State Battery Cathode with a Polymer Composite Electrolyte and Low Tortuosity Microstructure by Directional Freezing and Polymerization. *Adv. Energy Mater.* **2021**, *11*, 2002387. [CrossRef]
20. Haridas, A.K.; Huang, C. Advances in Strategic Inhibition of Polysulfide Shuttle in Room-Temperature Sodium-Sulfur Batteries via Electrode and Interface Engineering. *Batteries* **2023**, *9*, 223. [CrossRef]
21. Han, X.; Cai, J.; Wang, X.; Liu, Y.; Zhou, H.; Meng, X. Understanding Effects of Conductive Additives in Lithium-Sulfur Batteries. *Mater. Today Commun.* **2021**, *26*, 101934. [CrossRef]
22. Dong, L.; Liu, J.; Chen, D.; Han, Y.; Liang, Y.; Yang, M.; Yang, C.; He, W. Suppression of Polysulfide Dissolution and Shuttling with Glutamate Electrolyte for Lithium Sulfur Batteries. *ACS Nano* **2019**, *13*, 14172–14181. [CrossRef]
23. Wang, Z.; Ji, H.; Zhou, L.; Shen, X.; Gao, L.; Liu, J.; Yang, T.; Qian, T.; Yan, C. All-Liquid-Phase Reaction Mechanism Enabling Cryogenic Li–S Batteries. *ACS Nano* **2021**, *15*, 13847–13856. [CrossRef]
24. Yu, L.; Ong, S.J.H.; Liu, X.; Mandler, D.; Xu, Z.J. The Importance of the Dissolution of Polysulfides in Lithium-Sulfur Batteries and a Perspective on High-Energy Electrolyte/Cathode Design. *Electrochim. Acta* **2021**, *392*, 139013. [CrossRef]
25. Ren, W.; Ma, W.; Zhang, S.; Tang, B. Recent Advances in Shuttle Effect Inhibition for Lithium Sulfur Batteries. *Energy Storage Mater.* **2019**, *23*, 707–732. [CrossRef]
26. Chung, S.H.; Manthiram, A. Lithium–Sulfur Batteries with the Lowest Self-Discharge and the Longest Shelf Life. *ACS Energy Lett.* **2017**, *2*, 1056–1061. [CrossRef]
27. Chien, Y.C.; Lacey, M.J.; Steinke, N.J.; Brandell, D.; Rennie, A.R. Correlations between Precipitation Reactions and Electrochemical Performance of Lithium-Sulfur Batteries Probed by Operando Scattering Techniques. *Chem* **2022**, *8*, 1476–1492. [CrossRef]
28. Guo, J.; Liu, J. A Binder-Free Electrode Architecture Design for Lithium–Sulfur Batteries: A Review. *Nanoscale Adv.* **2019**, *1*, 2104–2122. [CrossRef]
29. Zhou, L.; Danilov, D.L.; Qiao, F.; Wang, J.; Li, H.; Eichel, R.A.; Notten, P.H.L. Sulfur Reduction Reaction in Lithium–Sulfur Batteries: Mechanisms, Catalysts, and Characterization. *Adv. Energy Mater.* **2022**, *12*, 2202094. [CrossRef]
30. Wu, Y.; Jin, T.; Momma, T.; Yokoshima, T.; Nara, H.; Osaka, T. Potentiostatic Way to Fabricate Li2Sx Cathode with Suppressed Polysulfide Formation. *J. Power Sources* **2018**, *399*, 287–293. [CrossRef]
31. Safdar, T.; Huang, C. Sulfur/Carbon Cathode Material Chemistry and Morphology Optimisation for Lithium–Sulfur Batteries. *RSC Adv.* **2024**, *14*, 30743–30755. [CrossRef]
32. Fahad, S.; Wei, Z.; Kushima, A. In-situ TEM observation of fast and stable reaction of lithium polysulfide infiltrated carbon composite and its application as a lithium sulfur battery electrode for improved cycle lifetime. *J. Power Sources* **2021**, *506*, 230175.
33. Pozio, A.; Di Carli, M.; Aurora, A.; Falconieri, M.; Della Seta, L.; Prosini, P.P. Hard Carbons for Use as Electrodes in Li-S and Li-ion Batteries. *Nanomaterials* **2022**, *12*, 1349. [CrossRef]

34. Wang, M.; Xia, X.; Zhong, Y.; Wu, J.; Xu, R.; Yao, Z.; Wang, D.; Tang, W.; Wang, X.; Tu, J. Porous Carbon Hosts for Lithium–Sulfur Batteries. *Chem. Eur. J.* **2019**, *25*, 3710–3725. [CrossRef]
35. Rao, M.; Li, W.; Cairns, E.J. Porous Carbon-Sulfur Composite Cathode for Lithium/Sulfur Cells. *Electrochem. Commun.* **2012**, *17*, 1–5. [CrossRef]
36. Takahashi, T.; Yamagata, M.; Ishikawa, M. A Sulfur–Microporous Carbon Composite Positive Electrode for Lithium/Sulfur and Silicon/Sulfur Rechargeble Batteries. *Prog. Nat. Sci. Mater. Int.* **2015**, *25*, 612–621. [CrossRef]
37. Tonoya, T.; Hinago, H.; Ishikawa, M. Development of Highly Sulfur-Loadable Microporous Activated Carbon from Azulmic Acid for Lithium-Sulfur Battery. In *Electrochemical Society Meeting Abstracts prime2020*; The Electrochemical Society, Inc.: Pennington, NJ, USA, 2020; MA2020-02; p. 3454. [CrossRef]
38. Tonoya, T.; Matsui, Y.; Hinago, H.; Ishikawa, M. Microporous Activated Carbon Derived from Azulmic Acid Precursor with High Sulfur Loading and Its Application to Lithium-Sulfur Battery Cathode. *Electrochem. Commun.* **2022**, *140*, 107333. [CrossRef]
39. Wang, T.; He, J.; Cheng, X.B.; Zhu, J.; Lu, B.; Wu, Y. Strategies toward High-Loading Lithium–Sulfur Batteries. *ACS Energy Lett.* **2022**, *8*, 116–150. [CrossRef]
40. Pan, H.; Huang, X.; Zhang, R.; Zhang, T.; Chen, Y.; Hoang, T.K.A.; Wen, G. Reduced Graphene Oxide-Encapsulated Mesoporous Silica as Sulfur Host for Lithium–Sulfur Battery. *J. Solid State Electrochem.* **2018**, *22*, 3557–3568. [CrossRef]
41. Zhang, H.; Yu, S. 20—Impedance Humidity Sensors Based on Metal Oxide Semiconductors: Characteristics and Mechanism. In *Modeling, Characterization, and Production of Nanomaterials*, 2nd ed.; Tewary, V.K., Zhang, Y., Eds.; Woodhead Publishing Series in Electronic and Optical Materials; Woodhead Publishing: Sawston, UK, 2023; pp. 549–580. [CrossRef]
42. Zhao, J. Capillary Force and Surface Wettability. In *Encyclopedia of Tribology*; Wang, Q.J., Chung, Y.W., Eds.; Springer: Boston, MA, USA, 2013; pp. 295–298. [CrossRef]
43. Lin, H.; Yang, L.; Jiang, X.; Li, G.; Zhang, T.; Yao, Q.; Zheng, G.W.; Lee, J.Y. Electrocatalysis of Polysulfide Conversion by Sulfur-Deficient MoS2 Nanoflakes for Lithium–Sulfur Batteries. *Energy Environ. Sci.* **2017**, *10*, 1476–1486. [CrossRef]
44. Zhao, W.M.; Shen, J.D.; Xu, X.J.; He, W.X.; Liu, L.; Chen, Z.H.; Liu, J. Functional Catalysts for Polysulfide Conversion in Li–S Batteries: From Micro/Nanoscale to Single Atom. *Rare Met.* **2022**, *41*, 1080–1100. [CrossRef]
45. Wu, L.; Hu, J.; Yang, X.; Liang, Z.; Chen, S.; Liu, L.; Hou, H.; Yang, J. Synergistic Effect of Adsorption and Electrocatalysis of CoO/NiO Heterostructure Nanosheet Assembled Nanocages for High-Performance Lithium–Sulfur Batteries. *J. Mater. Chem. A* **2022**, *10*, 23811–23822. [CrossRef]
46. Azam, S.; Wei, Z.; Wang, R. Cerium Oxide Nanorods Anchored on Carbon Nanofibers Derived from Cellulose Paper as Effective Interlayer for Lithium Sulfur Battery. *J. Colloid Interface Sci.* **2022**, *615*, 417–431. [CrossRef]
47. Liu, Y.; Liu, H.; Tian, L.; Pang, L.; Liu, X.; Li, J. Synergic Adsorption and Catalytic Conversion of Polysulfides Based on Polar Mo2C and Pyridinic N for the Enhanced Electrochemical Performance of Li–S Batteries. *Mater. Today Sustain.* **2022**, *18*, 100155. [CrossRef]
48. Gao, X.T.; Zhu, X.D.; Gu, L.L.; Wang, C.; Sun, K.N.; Hou, Y.L. Efficient Polysulfides Anchoring for Li-S Batteries: Combined Physical Adsorption and Chemical Conversion in V2O5 Hollow Spheres Wrapped in Nitrogen-Doped Graphene Network. *Chem. Eng. J.* **2019**, *378*, 122189. [CrossRef]
49. Zhang, K.; Chen, F.; Pan, H.; Wang, L.; Wang, D.; Jiang, Y.; Wang, L.; Qian, Y. Study on the Effect of Transition Metal Sulfide in Lithium–Sulfur Battery. *Inorg. Chem. Front.* **2019**, *6*, 477–481. [CrossRef]
50. Park, Y.Y.; Moon, S.H.; Park, D.H.; Shin, J.H.; Kim, J.H.; Jang, J.S.; Kim, S.B.; Lee, S.N.; Park, K.W. Vanadium Nitride/Reduced Graphene Oxide Composite Interlayer with Dual Lithium-Polysulfide Adsorption Effect for Lithium-Sulfur Batteries. *J. Alloys Compd.* **2023**, *960*, 170812. [CrossRef]
51. Wei, Z.; Sarwar, S.; Azam, S.; Ahasan, M.R.; Voyda, M.; Zhang, X.; Wang, R. Ultrafast Microwave Synthesis of $MoTe_2$@graphene Composites Accelerating Polysulfide Conversion and Promoting Li_2S Nucleation for High-Performance Li-S Batteries. *J. Colloid Interface Sci.* **2023**, *635*, 391–405. [CrossRef]
52. Yuan, B.; Zhao, J.; Liu, W.; Liu, H.; Chen, P.; Sun, L.; Guo, X.; Wang, X.; Zhang, W.; Zhang, R.; et al. Preparation and Application of NiS2/NiSe2 Heterostructure as a Sulfur Host in Lithium-Sulfur Batteries. *J. Alloys Compd.* **2024**, *987*, 174231. [CrossRef]
53. Li, Y.; Hao, Y.; Ali, U.; Zhang, Q.; Jin, Z.; Sun, H.; Li, L.; Zhang, L.; Wang, C.; Liu, B. Bimetallic Sulfides Heterostructure Efficient Adsorption and Catalytic of Polysulfides for High-Performance Lithium-Sulfur Batteries. *Chem. Eng. J.* **2023**, *474*, 145961. [CrossRef]
54. Gao, D.; Li, Y.; Guo, Z.; Liu, Z.; Guo, K.; Fang, Y.; Xue, Y.; Huang, Y.; Tang, C. Sc2CO-MXene/h-BN Heterostructure with Synergetic Effect as an Anchoring and Catalytic Material for Lithium-Sulfur Battery. *J. Alloys Compd.* **2021**, *887*, 161273. [CrossRef]
55. Wang, J.; Zhou, L.; Guo, D.; Wang, X.; Fang, G.; Chen, X.; Wang, S. Flower-Like NiS2/WS2 Heterojunction as Polysulfide/Sulfide Bidirectional Catalytic Layer for High-Performance Lithium-Sulfur Batteries. *Small* **2023**, *19*, 2206926. [CrossRef]
56. Liu, X.; Huang, J.Q.; Zhang, Q.; Mai, L. Nanostructured Metal Oxides and Sulfides for Lithium–Sulfur Batteries. *Adv. Mater.* **2017**, *29*, 1601759. [CrossRef]

57. Zhang, B.; Ma, J.; Cui, M.; Zhao, Y.; Wei, S. A Rational Design of a CoS2-CoSe2 Heterostructure for the Catalytic Conversion of Polysulfides in Lithium-Sulfur Batteries. *Materials* **2023**, *16*, 3992. [CrossRef]
58. Chang, Z.; Liu, W.; Feng, J.; Lin, Z.; Shi, C.; Wang, T.; Lei, Y.; Zhao, X.; Song, J.; Wang, G. Cobalt/MXene-derived TiO_2 Heterostructure as a Functional Separator Coating to Trap Polysulfide and Accelerate Redox Kinetics for Reliable Lithium-sulfur Battery. *Batter. Supercaps* **2024**, *7*, e202300516. [CrossRef]
59. Zhao, Z.; Yi, Z.; Duan, Y.; Pathak, R.; Cheng, X.; Wang, Y.; Elam, J.W.; Wang, X. Regulating the D-p Band Center of FeP/Fe2P Heterostructure Host with Built-in Electric Field Enabled Efficient Bidirectional Electrocatalyst toward Advanced Lithium-Sulfur Batteries. *Chem. Eng. J.* **2023**, *463*, 142397. [CrossRef]
60. Zheng, M.; Zhao, J.; Wu, W.; Chen, R.; Chen, S.; Cheng, N. Co/CoS2 Heterojunction Embedded in N, S-Doped Hollow Nanocage for Enhanced Polysulfides Conversion in High-Performance Lithium–Sulfur Batteries. *Small* **2024**, *20*, 2303192. [CrossRef]
61. Zhu, C.; Zhou, W.; Chen, M.; Yuan, K.; Chen, N.; Wang, A.; Zhao, D.; Li, L.; Liang, X.; An, M. N Doped Carbon Supported Cobalt/Tungsten Nitride Mott-Schottky Heterojunction as an Efficient Electrocatalyst to Enhance Adsorption and Conversion of Lithium Polysulfides for High-Performance Lithium–Sulfur Batteries. *Electrochim. Acta* **2024**, *489*, 144184. [CrossRef]
62. Peng, L.; Wei, Z.; Wan, C.; Li, J.; Chen, Z.; Zhu, D.; Baumann, D.; Liu, H.; Allen, C.S.; Xu, X.; et al. A fundamental look at electrocatalytic sulfur reduction reaction. *Nat. Catal.* **2020**, *3*, 762–770.
63. Zhang, W.; Li, Y.; Lv, H.; Xie, S.; Zhu, J.; Xu, J.; Jin, H.; Kong, X.; Jin, S.; Wang, H.; et al. A comparison study of the electrocatalytic sulfur reduction activity on heteroatom-doped graphene for Li–S battery. *Small Struct.* **2023**, *4*, 2200244.
64. Cui, Y.; Fang, W.; Zhang, J.; Li, J.; Wu, H.; Sun, Z.; Cai, Y.; Zhang, H.; Zhang, S. Controllable sulfur redox multi-pathway reactions regulated by metal-free electrocatalysts anchored with LiS3* radicals. *Nano Energy* **2024**, *122*, 109343. [CrossRef]
65. Shen, J.; Liang, Z.; Gu, T.; Sun, Z.; Wu, Y.; Liu, X.; Liu, J.; Zhang, X.; Liu, J.; Shen, L.; et al. Revisiting the unified principle for single-atom electrocatalysts in the sulfur reduction reaction: From liquid to solid-state electrolytes. *Energy Environ. Sci.* **2024**, *17*, 6034–6045.
66. Cai, G.; Lv, H.; Zhang, G.; Liu, D.; Zhang, J.; Zhu, J.; Xu, J.; Kong, X.; Jin, S.; Wu, X.; et al. A Volcano Correlation between Catalytic Activity for Sulfur Reduction Reaction and Fe Atom Count in Metal Center. *J. Am. Chem. Soc.* **2024**, *146*, 13055–13065.
67. Shou, H.; Zhou, Q.; Wei, S.; Liu, H.; Lv, H.; Wu, X.; Song, L. High-Throughput Screening of Sulfur Reduction Reaction Catalysts Utilizing Electronic Fingerprint Similarity. *JACS Au* **2024**, *4*, 930–939. [PubMed]
68. Rakhimol, K.R.; Kalarikkal, N.; Thomas, S. Different Types of Separators for Lithium Sulfur Battery. In *Nanostructured Materials for Lithium/Sulfur Batteries*; Gueye, A.B., Thomas, S., Eds.; Springer International Publishing: Berlin/Heidelberg, Germany, 2024; pp. 431–444. . [CrossRef]
69. Ouellette, R.J.; Rawn, J.D. 1—Structure of Organic Compounds. In *Principles of Organic Chemistry*; Ouellette, R.J., Rawn, J.D., Eds.; Elsevier: Amsterdam, The Netherlands, 2015; pp. 1–32. [CrossRef]
70. Lin, J.; Zhang, K.; Zhu, Z.; Zhang, R.; Li, N.; Zhao, C. CoP/C Nanocubes-Modified Separator Suppressing Polysulfide Dissolution for High-Rate and Stable Lithium–Sulfur Batteries. *ACS Appl. Mater. Interfaces* **2019**, *12*, 2497–2504. [CrossRef] [PubMed]
71. Lee, J.H.; Kang, J.; Kim, S.W.; Halim, W.; Frey, M.W.; Joo, Y.L. Effective Suppression of the Polysulfide Shuttle Effect in Lithium–Sulfur Batteries by Implementing rGO–PEDOT:PSS-Coated Separators via Air-Controlled Electrospray. *ACS Omega* **2018**, *3*, 16465–16471. [CrossRef]
72. Tang, Q.; Li, H.; Pan, Y.; Zhang, J.; Lin, Z.; Chen, Y.; Shu, X.; Qi, W. TiN Synergetic with Micro-/Mesoporous Carbon for Enhanced Performance Lithium–Sulfur Batteries. *Ionics* **2018**, *24*, 2983–2993. [CrossRef]
73. Hong, X.; Jin, J.; Wen, Z.; Zhang, S.; Wang, Q.; Shen, C.; Rui, K. On the Dispersion of Lithium-Sulfur Battery Cathode Materials Effected by Electrostatic and Stereo-Chemical Factors of Binders. *J. Power Sources* **2016**, *324*, 455–461. [CrossRef]
74. Niu, C.; Liu, J.; Qian, T.; Shen, X.; Zhou, J.; Yan, C. Single Lithium-Ion Channel Polymer Binder for Stabilizing Sulfur Cathodes. *Natl. Sci. Rev.* **2020**, *7*, 315–323. [CrossRef]
75. Huang, Y.; Shaibani, M.; Gamot, T.D.; Wang, M.; Jovanović, P.; Dilusha Cooray, M.C.; Mirshekarloo, M.S.; Mulder, R.J.; Medhekar, N.V.; Hill, M.R.; et al. A Saccharide-Based Binder for Efficient Polysulfide Regulations in Li-S Batteries. *Nature Commun.* **2021**, *12*, 5375. [CrossRef]
76. Liao, J.; Liu, Z.; Wang, J.; Ye, Z. Cost-Effective Water-Soluble Poly(Vinyl Alcohol) as a Functional Binder for High-Sulfur-Loading Cathodes in Lithium–Sulfur Batteries. *ACS Omega* **2020**, *5*, 8272–8282. [CrossRef]
77. Qin, T.; Yang, H.; Li, Q.; Yu, X.; Li, H. Design of Functional Binders for High-Specific-Energy Lithium-Ion Batteries: From Molecular Structure to Electrode Properties. *Ind. Chem. Mater.* **2024**, *2*, 191–225. [CrossRef]
78. Zhou, G.; Liu, K.; Fan, Y.; Yuan, M.; Liu, B.; Liu, W.; Shi, F.; Liu, Y.; Chen, W.; Lopez, J.; et al. An Aqueous Inorganic Polymer Binder for High Performance Lithium–Sulfur Batteries with Flame-Retardant Properties. *ACS Cent. Sci.* **2018**, *4*, 260–267. [CrossRef]
79. Han, P.; Chung, S.H.; Chang, C.H.; Manthiram, A. Bifunctional Binder with Nucleophilic Lithium Polysulfide Immobilization Ability for High-Loading, High-Thickness Cathodes in Lithium–Sulfur Batteries. *ACS Appl. Mater. Interfaces* **2019**, *11*, 17393–17399. [CrossRef] [PubMed]

80. Li, G.; Ling, M.; Ye, Y.; Li, Z.; Guo, J.; Yao, Y.; Zhu, J.; Lin, Z.; Zhang, S. Acacia Senegal–Inspired Bifunctional Binder for Longevity of Lithium–Sulfur Batteries. *Adv. Energy Mater.* **2015**, *5*, 1500878. [CrossRef]
81. Sun, Q.; He, B.; Zhang, X.Q.; Lu, A.H. Engineering of Hollow Core–Shell Interlinked Carbon Spheres for Highly Stable Lithium–Sulfur Batteries. *ACS Nano* **2015**, *9*, 8504–8513. [CrossRef]
82. Bai, Y.; Nguyen, T.T.; Chu, R.; Kim, N.H.; Lee, J.H. Core-Shell Hollow Nanostructures as Highly Efficient Polysulfide Conversion and Adsorption Cathode for Shuttle-Free Lithium-Sulfur Batteries. *Chem. Eng. J.* **2023**, *454*, 140338. [CrossRef]
83. Li, S.; Fan, Z. Encapsulation Methods of Sulfur Particles for Lithium-Sulfur Batteries: A Review. *Energy Storage Mater.* **2023**, *34*, 107–127. [CrossRef]